DEVELOPMENT OF A HIGH ACCURACY SUN SENSOR FOR THE GEO-STATIONARY METEOROLOGY SATELLITE

LI Yong-Fu[1)] CHEN Gui-Lin[2)]

([1)]Xiamen Municipal Bureau of Information Industry, Xiamen, Fujian 361012, China;
[2)]Shanghai Institute of Technical Physics, Chinese Academy of Sciences, Shanghai 200083, China)

Abstract Basing upon the requirements of the scanning synchronization controller system of the geo-stationary meteorology satellite (GSMS) and the characteristics of the solar target, a prototype of on-board high accuracy sun sensor (HASS) and a set of testing equipment of this HASS has been developed. The designed sun sensor, which is used on the GSMS both for the scanning synchronization controller and for the alignment guiding of cloud pictures at earth stations, has two pairs of slits and uses an equivalent detection method to generate a high accuracy sun pulse. It has realized a measuring accuracy of 0.46 microseconds (r. m. s) when the satellite rotates at a rate of 100 r/min in the sector meridian plane of the satellite ranging from −29.5° to +29.5°. In addition, the sensor has the characteristics of high reliability, real-time and low power consumption.
Key words sun sensor, double-slit detector, equivalent detection method, geo-stationary meteorology satellite.

地球同步气象卫星星载高精度太阳敏感器的研制

李永福[1)] 陈桂林[2)]

([1)]厦门市信息产业局,福建,厦门,361012;
[2)]中国科学院上海技术物理研究所,上海,200083)

摘要 根据地球同步气象卫星(GSMS)星载扫描同步控制器系统的要求和对太阳目标特性的分析,研制了一台用于该 GSMS 的星载高精度太阳敏感器(HASS)及配套的性能测试装置.该太阳敏感器的光学头部由两对狭缝组成,采用平衡检测方式产生高精度的太阳脉冲,为星上扫描同步控制器和卫星地面站云图配准的引导提供基准信号.其在卫星子午面内的扇形视场为 −29.5° ~ +29.5°,当其随星体按 100r/min 的速率旋转时,可实现 0.46μs(r. m. s)的测量精度.另外,该太阳敏感器还具有高可靠性、实时性和低功耗的特点.
关键词 太阳敏感器,双缝式探测器,平衡检测方法,地球同步气象卫星.

Introduction

The high accuracy sun sensor (HASS) presented in this paper is developed on the basis of the application requirements of the geo-stationary meteorology satellite (GSMS), which is located on the equatorial plane of the earth and spins around its axis at a rate of 100r/min. An on-board multi-channel scanning radiometer (MCSR), rotating with the satellite, has a telescope system which moves step by step along the south-north direction in the meridian plane of the satellite. The MCSR scans the earth disc in an angular range of 20° × 20° to obtain cloud pictures of the earth. Since the instantaneous field of view (IFOV) of the MCSR is very small, such as 35 × 35 $(\mu r)^2$ for each image element of visible channel, a whole cloud image got by the GSMS is composed of 10000 visible data lines or 2500 infrared data lines correspondingly.

Received 2001 - 08 - 27, revised 2003 - 01 - 02

稿件收到日期 2001 - 08 - 27, 修改稿收到日期 2003 - 01 - 02

In order to obtain a perfect cloud image on the satellite and to restore it at earth stations precisely, a high accuracy standard signal is needed to accomplish the scanning synchronization control of the MCSR and to guide the data line alignment of the scanned cloud picture. The HASS, which provides the high accurate sun pulse(SP), has been developed for this definite purpose.

1 Operation principle

1.1 Characteristics of the solar target

The sun is the target directly detected by the HASS. Therefore, at the very beginning to study the solar physical characteristics and the relative orbiting movements of the sun, the earth and the GSMS is very helpful to design the sensor. After detailed analysis[1], the following has been concluded:

a) Since it takes 30 minutes for the GSMS to complete a whole scanning cycle, the sun sensor must remain steady measuring accuracy (in the order of angular seconds) in this period, the sun may be considered as an ideal uniform disc. This basic concept limits the accuracy of the sun sensor to the order of angular seconds because of the solar limb attributes and its activities (such as sunspots)[2-4].

b) In order to capture the sun target at any time in a year without tracing device, the sun sensor's angular field of view (FOV) in the meridian plane of satellite must be greater than $\pm 23.5°$.

c) The relative fluctuation of the solar constant in one year is about 6.7%[5], and the response of photo-detector varies with the changes of incident angle (the cosine law). These two facts result in the changes of the photo-detector's output amplitude.

1.2 Basic operation principle

In accordance with the application requirements of the GSMS stated above and the characteristics of the solar target, a double-slit sun sensor, which used the equivalent detection method, was designed. The sensor mainly consists of three parts, the optical head, detectors and electronic signal processing system. The optical system, which uses two incident slits, has a large fan beam FOV in the meridian plane of the GSMS and a narrow IFOV in the direction of scanning. When the sun comes present, the small IFOV increases the edge slope of detector outputs and ensures the measuring accuracy of the sun sensor. The following electronic circuit processes the electronic signals converted by the photosensitive detectors. Then an accurate sun pulse with a width of 2ms is generated. Being used as the scanning reference, the sun pulse is provided to the analogue phase-locked frequency multiplier and the sun angle correction circuit in the scanning synchronization controller. Then an equal-angle clock, which uses the earth as its reference, is converted from the SP by a synchronous signal generator. This clock synchronously controls the sequential actions of the MCSR at some fixed scanning positions. At the same time, the sun pulse is transmitted to the ground station through two channels, the analogue real-time remote sensing channel and the digital data transmitting channel, to provide the ground image processing system with a precise standard[6].

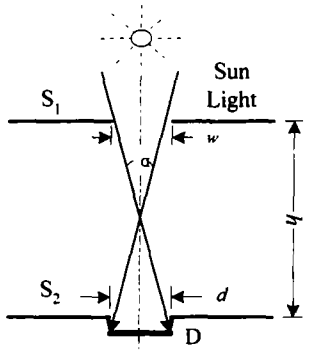

Fig. 1 Single-slit sun sensor
图 1 单缝式太阳敏感器

In order to explain the operation principle of the sun sensor, the analyzed single-slit sensor was shown in Fig. 1. The sensor consists of two parallel slits, the incident slit S_1, the masking slit S_2 and a detector adhering to the bottom surface of S_2. The IFOV of the sensor is $\alpha = 2\tan^{-1}(w+d)/2h$, where w and d are the widths of S_1 and S_2 respectively. h is the length of the collimator formed by S_1 and S_2. Since α is very small, $tan\ \alpha \approx \alpha$, then,

$$\alpha \approx (w+d)/h. \qquad (1)$$

The sensor uses the threshold detecting method to sense the presence of the sun. When the sensor on the spinning satellite scans the outer space, the sun

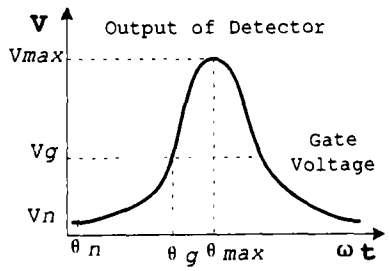

Fig. 2　Output signal of the detector
图 2　探测器的输出信号

will transit the IFOV of the sensor and make the detector produce a signal as shown in Fig. 2. When the sun is out of the IFOV of the sensor, a noise signal of amplitude V_n is produced by stray rays in space and 4°K cold background radiation. When the sun is on the central line of the sensor's IFOV, a maximum output V_{max} is produced. After being pre-amplified and removed from the interference of noise signal, the signal is used to compare with a fixed gate-voltage to generate a signal representing the presence of the sun. The accuracy of this method is determined by the edge slope of the signal, which is related to the solar characteristics and the sensor's IFOV α. Through detailed analysis, it can be inferred that the smaller the IFOV α, the more rapidly rising or dropping the output signal and the more accurate the sensing of the sun.

The principle of HASS is similar to that of the sensor stated above, but the HASS uses a new method, that is the equivalent detection using two pairs of slits. As shown in Fig. 3, the HASS is made up of two parallel incident slits (S_{11} and S_{12}), two FOV masking slits (S_{21} and S_{22}) and two detectors (D_1 and D_2). The two detectors D_1 and D_2 are adhered to the slits S_{21} and S_{22} respectively. Where slits S_{21} and S_{22}, at the bottom of

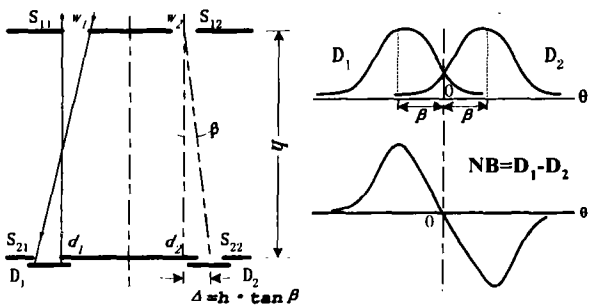

Fig. 3　Double-slit sun sensor and its NB signal
图 3　双缝式太阳敏感器及其非平衡信号

the collimator, are parallel to the two incident slits, while the central line of each masking slit has a displacement of Δ with respect to its corresponding incident slit. The four slits form a pair of single-slit sensors stated above, while the displacement Δ makes the outputs of detector D_1 and D_2 have a phase difference 2β. And then a non-balance quantity (NB) can be obtained by subtracting one signal from the other. When the sun is on the central line of the optical system, the solar energy amplitudes received by the two detectors are equal and the converted outputs reach to the balance point ($NB=0$). The electronic processing circuit detects this point and provides a sun pulse with represent the appearance of the sun. This is the basic principle of equivalent detection method used by a double-slit sun sensor.

The equivalent detection method not only doubles the signal sloping rate at zero point and increases the measuring accuracy of the sun sensor, but also resolves the contradiction between the amplitude variation of detector's output, which changes with the solar constant and the incident angle, and the fixed threshold. This contradiction cannot be overcome in a single-slit sun sensor. Furthermore, the new type sun sensor remains the advantages of single-slit sun sensor, such as simplicity, reliability, wide fan beam FOV, etc. This design concept makes it easy to acquire a real-time sun pulse for the satallite.

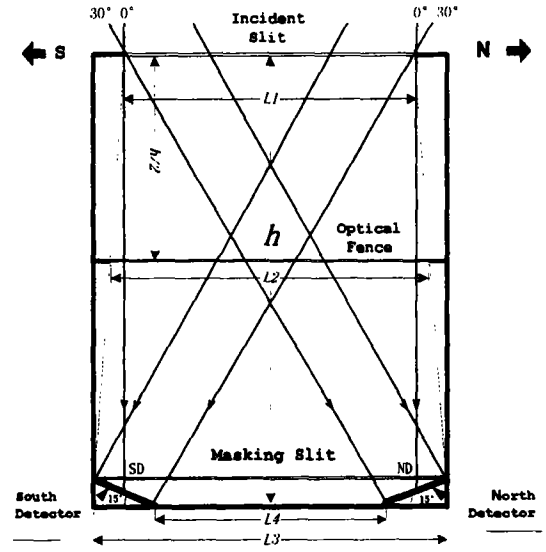

Fig. 4　Optical configuration of sun sensor
图 4　太阳敏感器的光学结构

2 Description of design

2.1 Set-up of optical system

Fig. 4 shows the optical configuration of HASS. The collimator length h and the slit length l are derived from the required dimension limitation. On the other hand, the slit widths d and w are determined by the relevant factors such as the IFOV of the sun sensor, the solar energy to receive (which affects the signal-noise ratio S/N) and the slit diffraction effect. Given h = 149mm, the delicately designed experiment shows the best solution, that is the width d, w and angle β should take the values of 0.2mm, 0.2mm and 10.4′ respectively. Therefore, $\Delta = h \cdot \tan\beta = 0.45$mm.

A pair of detectors called south detector and north detector are mounted under each of the two masking slits and their sensitive surfaces make a +15° or −15° angle with the normal of masking surface respectively. Each of the two detectors has a FOV of ±15°. The two detectors are parallel connected, as shown in Fig. 5, to form a united detector which has a large fan beam FOV of about ±30°. When the sun is on the central axis of the optical system, the north and south detectors are half illuminated. During one year, the sun changes its latitudinal position in the meridian plane of the satellite. However, the illuminated areas of the two detectors are compensated with each other to remain their sum keeping the same. Considering the cosine effect of detectors, the relative output variation of the connected detectors is less than 0.08% when the sun changes its position in the whole fan beam FOV of HASS[1]. Besides, the optical fence fixed at the middle of the collimator eliminates the multiple reflections and the interference of light rays from different incident slits. Without the need of changing the shape and dimensions of the sensor, a backup, or a spare part of the same optical system can be easily achieved. This is enough to increase the reliability.

The manufacture of these long narrow slits is completed by means of advanced photo-etching technique, which makes the un-parallelism between slits and that between the two edges of each slit less than 5μm. Furthermore, one pair of short etchings, which have an equal length of 10mm and are narrower than the slits, are etched together with the incident slits on the central line of sensor's front end. As the same, another pair of short etchings are etched together with the masking slits on the central line of sensor's rear end. These two etching pairs work as the base-line standard used to align the incident and masking slits. It is assured that the un-parallelism between the incident and masking slits is less than 1μm.

2.2 Detectors

The detectors chosen for the HASS are silicon solar cells. The reason is that Si solar cell has some advantages comparing with other photosensitive detectors. At first, the spectral response of Si solar cell lies in the wavelength range of 0.45 ~ 1.1μm, which approximates to the solar energy distribution spectrum. The high photo-electronic transforming rate makes it possible for us to utilize the solar energy effectively and to get a good ratio of S/N. Secondly, the Si solar cell has small photo integration and electronic storage effect because of the small p-n junction capacitance. This is beneficial to real-time signal processing. Moreover, Si cell is a solid-state electronic device with the quality of high reliability. Thus, it works well under bad conditions and is suitable for space task.

In accordance with the V-I characteristics of solar cells,

$$I = I_L - I_S \cdot [Exp(qV/kT) - 1]. \qquad (2)$$

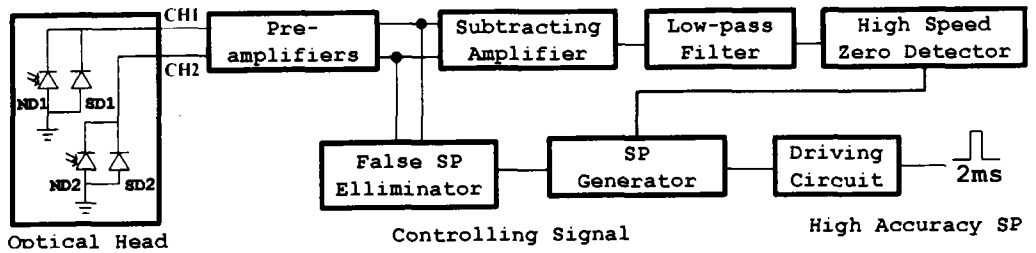

Fig. 5 Block diagram of signal processing system

图5 电子信号处理系统的方框图

where I_L is the short circuit current which is directly proportional to the solar energy received, I_S is the reversal saturation current of p-n junction, q is the charge quantity of an electron, k is the Boltzman constant, T is the absolute temperature, it can be inferred that when working in the optimum state of short-circuit, that is the load resistance $R_L \to 0$ and the bias voltage $V \to 0$, the Si cell outputs the short-circuit current $I_{SC} = I_L$, which is directly proportional to the solar irradiation. Besides, Si cell has small dark current I_D and p-n junction capacitance C_j. These properties effectively increase the S/N rate and responding speed of sun sensor.

2.3 Electronics

Fig. 5 shows the block diagram of the electronic processing part. The electronics uses the electronic signals generated by the solar cells in the optical head to produce a sun pulse (SP) of width $2ms$, and then provides it to the satellite. The electronics mainly includes six parts that are the preamplifiers, subtracting amplifier, filter circuit, high-speed zero detector, sun pulse generator and false SP eliminator, respectively. The preamplifiers are applied as current to voltage converters, which transform the photocurrent to voltage linearly. They are operational amplifiers with the qualities of ultra-low noise, high open-loop gain and input resistance, and work in a state of constant close-loop gain and deep negative feedback. This working state satisfies the optimum operating conditions required by photosensitive cells and the frequency bandwidth meets the requirement of signals. The non-balance quantity NB is derived from the amplified subtraction of the two preamplifier's outputs. This signal passes through a powered low-pass filter of bandwidth 11.5KHZ (at-3dB), which is composed of a first-order RC low-pass filter and a second-order Bessel low-pass filter. Using this kind of filter, we can make the signal group-delay remain constant in a wide range of frequency. When the zero detecting circuit meets the zero point of the filtered NB signal, a positive slope with rising time less than $20ns$ is generated. This slope triggers a multi-frequency oscillator in the SP generator circuit to generate the sun pulse of width 2ms. Since the NB signal is zero when the sun is out of the IFOV of the sun sensor, the output of zero detectors may accidentally trigger the oscillator to produce false sun pulses. Thus an additional circuit, which controls the generator, is designed to eliminate the false sun pulses.

Through theoretically analyzing the signal of the sensor system, we can know that the signal frequency bandwidth Δf is 1.94KHZ, and the signal to noise ratio S/N is approximately 14.3.

2.4 Error analysis

The measuring errors of the HASS can be classified as regular errors and random errors. All the errors come from four major sources, which are the attribute variations of solar surface, disfigurement of the mechanical and optical system, noise of detectors and signal processing error. Here the solar limb darkening effect has influence on the fringe characteristics of the sun, but only the intense solar activities, such as large sunspots, have an approximate 1″ contribution to the random errors. This determines the measuring precision limit of sun sensor if the sun is considered as a u-

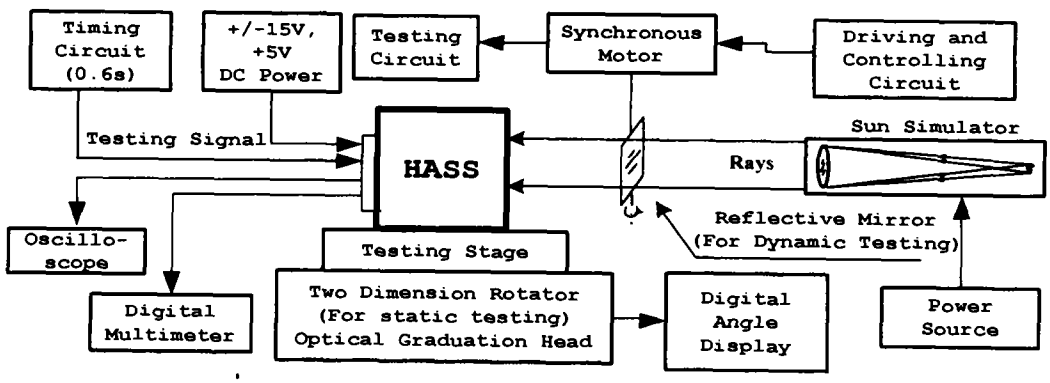

Fig. 6 Block diagram of testing equipment

图 6　太阳敏感器的测试装置

niform radiation disc. The errors induced from the mechanical and optical limitation can be calibrated or compensated. Using the signal to noise ratio S/N stated above, we can calculate the electronic signal processing error, which is less than 0.10μs.

3 Performance testing

Table 1 Specifications of HASS and requirements of GSMS
表1 太阳敏感器的技术特性与气象卫星要求的对照

Items	GSMS requirements	HASS specifications	Remarks
Number of sensor heads	1	1+1 (Spare part)	
Power consumption	1.0W	0.91W	DC sources: ±15V, +5V
Dimensions(mm)	180×120×60 (Sensor head)	172×109×133	Including the install base and electronics
Weights(Kg)	1.2 (Sensor head)	1.4	The electronic part weights only 0.163Kg
Accuracy	1μs (Dynamic)	σ≤0.46μs (Dynamic)	The equivalent static value is 1″
Fan beam FOV	≥±23.5°	±29.5°	
Output signal(SP)		Positive $V_{OL}<0.3V$, $V_{OH}>3.1V$	The sun pulse is driven by IC 54S140
Width of sun pulse	2 ms	2 ms	
Rising or falling slope of SP	t_r≤0.1μs	t_r≤0.1μs, t_f≤0.2μs	

In order to test the static and dynamic performance of HASS, a set of experiment equipments have been established, as shown in Fig. 6. The sun simulator, using a halogen-tungsten lamp as its light source, has an angular diameter of 32′. The simulator's brightness is 1/50 that of the sun and its stability is better than 0.1%. The two-dimension rotating stage, or optical graduation head, consists of two parts, the high accuracy (1″) grating graduation head and the digital angle display. We can use it to measure the static performance and the fan beam FOV of HASS. A reflective mirror mounted on the axis of a synchronous motor, which situates between the simulator and the sun sensor, is controlled by an electronic driving circuit. The motor of high stability rotates at a rate of 100r/min. The light reflected from the rotating mirror scans the sensor instead of the spinning of HASS, which makes the dynamic testing more easily. The digital angle pulses from the photo-electronic axis-angle encoder of the synchronous motor are processed in the testing circuit. This electronic circuit is especially designed to measure the accuracy of the sun pulse.

In Table 1 shows the major performance specifications of HASS and the requirements of the Geo-Stationary meteorology satellite. Some further experiments have been done with the MCSR and other parts of GSMS. Because of these tests, it is ensured that the designed HASS satisfies the application requirements of the GSMS.

4 Conclusion

The sun sensor, designed to produce a high accurate sun pulse for the GSMS, uses the double-slit optical configuration and the equivalent detection method to improve the measuring accuracy. It overcomes the shortages of fixed threshold detecting method used in a single-slit sun sensor. The HASS, which meets all the application specification requirements, has the attributes of high accuracy, wide fan beam FOV, real-time, reliability, etc. In addition, the HASS can also be used on a stabilized single-axis spinning satellite to measure its attitude and rotating speed.

REFERENCES

[1] LI Yong-Fu. Design of a high accuracy sun sensor for the GSMS: (Master Thesis). Shanghai: Shanghai Institute of Technical Physics, CAS. (李永福. 地球同步气象卫星用高精度太阳敏感器的研制. (硕士学位论文)中国科学院上海技术物理研究所,上海),1989

[2] Hammerschlag A, C W de Boom, H Bokhove. High accuracy sun sensor, final report phases IA and IB. *TPD Report*, 1977, **611.257**: 94—179

[3] Gutshall R L, Deters R A. A survey of attitude sensors (state of the art paper). *The Journal of the Astronautical Sciences*, 1979, **X X** Ⅶ(3): 217—238

[4] Wertz J R, ed. *Spacecraft Attitude Determination and Control.* Dordrecht: D. Reidel Publishing Company, 1979: 217—242

[5] Allen C W. *Astrophysical Quantities.* London: Athlone Press, 1981: 12

[6] SUN Mao-Heng. Data code buffer for multi-channel scanning radiometer on stationary meteosat. *Chinese Journal of Infrared and Millimeter Waves*, 1987,**6**: 249—254